Design of the Tri-band UWB Microstrip Patch Antenna for WBAN Applications

Kefa G. Mkongwa, Qingling Liu, and Chaozhu Zhang

College of Information and Communication Engineering
Harbin Engineering University, Harbin, 451 150000, China
ggkefa@gmail.com, liuqingling@hrbeu.edu.cn, zhangchaozhu@hrbeu.edu.cn

Abstract ─ The increasing commercialization of the Wireless Body Area Networks (WBAN) in various healthcare facilities poises for the growing network resources competition in the Physical layer. In remote health monitoring, energy scarcity and limited bandwidth compromise demand for optimized network lifetime and high data rate of the multimedia information with reduced spectral noises. In this paper, we have designed a compact Tri-band antenna with three rejection bands for WBAN applications. The rectangular antenna patch is etched on RT/Duroid substrate. The patch consists of flat chamfers, semi-circular, and elliptical slots. The simulated antenna resonates at three distinct frequencies; 6.39 GHz, 7.15 GHz, and 9.89 GHz each operating at the ultrawideband (UWB) with a return loss ($|S_{11}|$) > 10 dBm. The antenna is designed using Computer Simulation Technology software (CST-2016) and analyzed for its return loss, field radiation, bandwidth (cumulative BW, 3473.8 MHz), and voltage standing wave ratio (VSWR<1.5). Simulation results show antenna performance characteristics which suit various WBAN applications.

Index Terms ─ Data rate, frequency bands, Quality of Service (QoS), radiation patterns, return loss (S_{11}), Ultra-wideband (UWB), Voltage Stand Wave Ratio (VSWR), Wireless Body Area Networks (WBAN).

I. INTRODUCTION

Advances in research for Wireless sensor networks (WSN) envisaged the development of Wireless body area networks (WBAN). Currently, WBAN uses biological sensors for real-time remote health monitoring of the human body vital signs. Monitored physiological signs may include heart rate, blood pressure, blood sugar, blood oxygen concentration, ECG, and EEG among others [1-2]. The primary element of the WBAN is the wireless body sensor embedded with a miniaturized radiating antenna [3]. Biological sensors usually positioned in the body as implants or a wearable device are used to acquire physiological parameters for noninvasive medical diagnosis from the remote health facilities.

In the remote health facility, the accurate prognosis of the health situation depends on the quality of the received data. Although in the transmission media, data packets are highly impeded by several factors including anomalies as a result of packet collision, latency, energy scarcity, intrusion, interference, transmission link drop out and tissue-specific absorption rate (SAR) [4-5].

WBAN sensors are battery powered and are reportedly consuming more energy during transmission and detection of the wireless signals. Therefore, deployment of low power transceivers and power budget consideration during network design is necessary [6]. Sometimes, energy requirement and network resources management in WBAN depends on the nature of the monitored body organ. Since various body organs generate data with different rates, so communicating data with varying data rates demand compatible transmitters.

In this view, a significant volume of data in the transmission channel affects successful data delivery and reduced throughput due to interference, power and bandwidth limitation of the network infrastructure [7-9]. As far as network resource competition in WBAN is increasing in parallel with its commercialization, in this work, we have proposed a multi-band UWB antenna which resonates at three distinct frequencies to support higher data rates with minimal spectral noises and operational power requirement.

The contribution of this work focus on the design of the compact and low cost Tri-band UWB microstrip patch antenna with a reduced size by ~25% of the analytical design, isolation of the rejection bands using slots and cuts which subsequently enhanced impedance matching and, bandwidth enhancement whereas distinct operational bands support bandwidth >500 MHz each.

The organization of this work consists of five sections; Section I gives the introduction about WBAN network requirement, Section II briefs about UWB antennas, Section III discusses the materials and antenna design methods, Section IV discusses simulation results,

Submitted On: October 12, 2018
Accepted On: April 6, 2019

findings, and Section V conclude our work.

II. ULTRA-WIDEBAND ANTENNAS

Rising demand for eHealth multimedia services and future generation communication inquires broader bandwidth in the transmission channel. Since IEEE 802.15.6 standard for WBAN supports UWB spectrum in its PHY layer, the enormous demand for higher data rates in the wireless channel influence UWB antenna design for various QoS aware healthcare applications [10-11]. One of the characteristics of the PHY layer channels includes the bandwidth of ~500MHz and a data rate between 971.4Kbps - 15.6 MHz. Antennas supporting channel bandwidth greater than 500MHz (BW>=0.5GHz) or with a percent bandwidth of more than 20% are said to operate in the UWB spectrum [12].

UWB antennas have merits including; low power consumption, support for higher data rates and low interference probabilities. These features make UWB suitable for both Personal area networks (PAN) and BAN [13-14]. The UWB spectrum (3.1 - 10.6 GHz) support a range of wireless applications (e.g., radars and satellites) which ease WBAN mobile ambulatory services depending on the country of implementation [15].

Microstrip patch, unlike conventional antenna, is conformal; it can be deformed into different shapes and geometries to meet UWB application flexibility using notches [16]. Antenna notches are implemented through bending or introducing slots on the patch and ground plane; this alters its radiation characteristics and impendence matching. Notched antennas limit radio frequency interference at specific frequency bands. The significance of using slots in Notched antennas is to isolate interfering frequencies from operational frequency bands [17]. Slotted patch has existed in different shapes like a spearhead, U, E, H, F, PIFA slots and spiral antennas with distinct mechanisms of feeding. Various slitting techniques, use of thick substrate, stacked patch and parasitic elements have proven to improve bandwidth, radiation efficiency, gain and minimize scattering parameters [18-21].

Numerous research findings propose different design materials and recommend a minimum requirement to ensure better gain and minimum return loss while meeting body compatibility [22]. Authors in [23-24], suggests that WBAN antenna must be durable and portable for body implants and wearables with lower Specific Absorption Rate (SAR) for personal radiation safety.

Single band UWB signals (3.1-10.6 GHz), can be interfered by Wireless Local Area Network (WLAN, 5.2 - 5.8 GHz), and X-Band (7.25 - 8.4 GHz) for satellite communications which exist within UWB spectrum hence threatening data security and quality of service [25]. To avoid such impeding issues implementation of the multi-band UWB is necessitated.

To achieve minimal spectrum noises and low power requirement in the transmission channel, this work, used similar design criteria as in ([9]) and ([12]) to design an antenna with hybrid characteristics. We have introduced flat chamfers and circular cuts on the patch and an aperture on the ground plane to design an ultra wideband (UWB) microstrip patch antenna using Finite Difference Time Domain (FDTD).

III. MATERIALS AND DESIGN METHODS

The proposed rectangular Microstrip patch antenna is designed using lossy RT/duroid® 5880LZ substrate with dielectric constant and loss tangent (Tanô) of 1.96 and 0.0019 respectively as shown in Fig. 1. We preferred RT/Duroid due to its low cost, low moisture absorption, wide operating temperature range (-55ºC - 260ºC), excellent chemical resistance and uniform electrical properties over the frequency band [26]. We use Annealed copper with a thickness of 0.035mm in both radiating surfaces (patch) and a background plane.

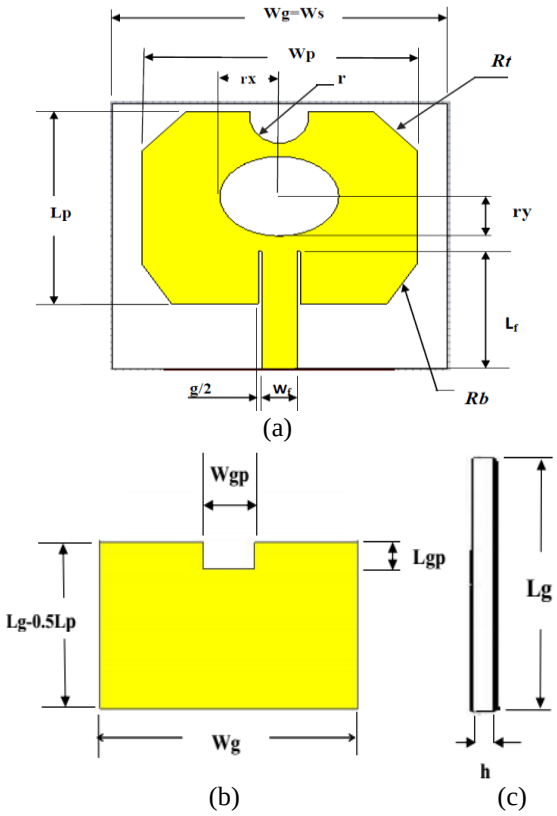

Fig. 1. Proposed antenna structure, (a) front view; consisting of patch and substrate dimensions. (b) Back view (ground plane); including the height of the ground plane and the narrow slot dimensions (c) side view.

Table 1: Antenna dimensions

Dimensions (mm)			Dimensions (mm)		
Parameter	**Calculated (initial)**	**Proposed**	**Parameter**	**Calculated (initial)**	**Proposed**
L_p	42.77	29	N_d	12.34	7.87
W_p	50.33	37	W_{gp}	-	9
L_s	52.73	40	L_{gp}	-	0.5
W_s	60.29	45	R_b	-	$4.7*45^0$
L_g	52.73	40	R_t	-	$6*45^0$
W_g	60.29	45	r_x	-	8
W_f	4.164	4.7	r_y	-	6
L_f	22.291	17.69	h	1.66	1.66
g	1	0.9	r		4

A. Mathematical modeling

An antenna was initially designed to resonate at 3.1 GHz, with a height of substrate (h=1.66). Other antenna dimensions were calculated using the following equations as stipulated in [27-28]. Patch width and length were obtained using equations (1) and (2):

$$W_P = \frac{c}{2 * f_r * \sqrt{\frac{\varepsilon_r + 1}{2}}}, \tag{1}$$

Where $\boldsymbol{c}$ is the speed of the electromagnetic wave in free space, $\boldsymbol{\varepsilon_r}$ is the permittivity in free space and $\boldsymbol{f_r}$ is the antenna resonant frequency.

Length of the patch is affected by fringing fields due to varying dielectric constant when electric fields propagate between air and substrate material along with radiating surfaces. Fringing fields results into the incremented length of the patch by 2*ôL; actual patch length is determined based on the effective length as follows:

$$L_p = L_{eff} - 2\partial L. \tag{2}$$

Where,

$$\varepsilon_{reff} = \frac{\varepsilon_r + 1}{2} + \frac{\varepsilon_r - 1}{2}\left[1 + 12\frac{h}{w_p}\right]^{-0.5}, \tag{3}$$

$$L_{eff} = \frac{c}{2 * f_r * \sqrt{\varepsilon_{reff}}}, \tag{4}$$

$$\partial L = 0.412 * h\left[\frac{\varepsilon_{reff} + 0.3}{\varepsilon_{reff} - 0.258}\right]\left[\frac{\frac{w_p}{h} + 0.264}{\frac{w_p}{h} + 0.8}\right]. \tag{5}$$

Equations (6) and (7) evaluates the length and width of the substrate:

$$L_s = L_p + 6h, \tag{6}$$

$$W_s = W_p + 6h, \tag{7}$$

Length of the microstrip feed line is obtained using equation (8):

$$L_f = \frac{c}{4 * f_r * \sqrt{\varepsilon_{reff}}}. \tag{8}$$

Table 1 shows calculated and proposed antenna dimensions respectively. Antenna dimensions were modified to meet minimum size requirements and operational frequency bands.

B. Design modification

In this work, we use hybrid design criteria as applied in the papers presented by Award et al. ([9]) and Turkmen et al. ([12]). In our design, we only considered methods used for bandwidth enhancement with some alteration of the design approach and materials. In [9], authors enhanced antenna bandwidth using round step cuts on the patch with similar dimensions while in our work, we introduced flat chamfer with different sizes on the edges of the radiating planes as illustrated in Table 1 ($\boldsymbol{R_t > R_b}$).

The implementation of the flat chamfers, round cut and the elliptical slot on the patch extended antenna radiation surface as shown in Fig. 2 (a), therefore apart from enhancing the bandwidth of the remaining frequency bands it also eliminated frequencies in the narrowband spectrum. The impact of slots and chamfers formed three notch bands between 0 - 6.12 GHz, 6.8 - 6.9 GHz and 8 - 9.47 GHz respectively.

Since the antenna could not resonate at UWB in all the frequency bands, we introduced a narrow slot on the ground plane as proposed by [12] to further extend operational antenna bandwidth and S_{11} far below -10dB. The antenna structure in Fig. 2 (b) shows the proposed antenna ground plane reduced by half the patch length (Lg-0.5Lp) with a narrow slot of dimensions Wgp*Lgp mm^2.

In practical application, WBAN requires smaller antenna size. Whereas, using lower permittivity substrate results into larger size antenna. This work focused on a well performing, compact and portable antenna. Therefore both substrate and patch dimensions were scaled down

by ~25% of the original design as demonstrated in Table 1. The proposed antenna dimensions were 40×45×1.66 mm^3 for the substrate.

IV. SIMULATION RESULTS

We ran simulations using Computer Simulation Technology (CST-2016) software. Simulation of the proposed antenna considered essential performance parameters including far-field radiation patterns, reflection coefficient and voltage standing wave ratio on free space.

After simulation, three sharp narrow troughs deep below -10dB at 6.39 GHz, 7.15 GHz, and 9.89 GHz were obtained. The three narrow, deep points of the S_{11} proves that the proposed antenna is a Tri-band resonating at three distinct frequencies.

A. Radiation patterns

Antenna E and H-field radiation patterns were simulated as shown in Fig. 2 and 3. Figure 2 (a) shows electric surface current on the patch, where higher field intensities (dB) indicated in yellow concentrates on the patch edges, notch gap, semicircular and elliptical slot.

During simulation, setting a narrow notch gap widened the operational bandwidth with gradual distortion on antenna return loss. Similarly, a thin slot at the middle of the ground plane was introduced. Figure 2 (b) demonstrates the impact of a narrow slot in the ground plane to the antenna field radiation patterns. A slight variation of the size of the aperture in the background plane highly contributed to the bandwidth enhancement of the antenna. 2D radiation patterns of the antenna are as shown in Fig. 3.

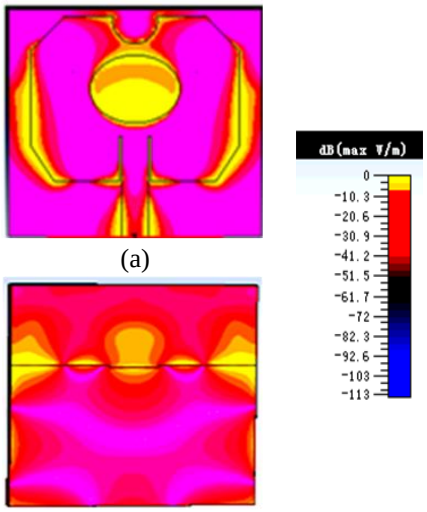

(a)

(b)

Fig. 2. E-Field distribution (a) on the patch, and (b) on the background plane respectively.

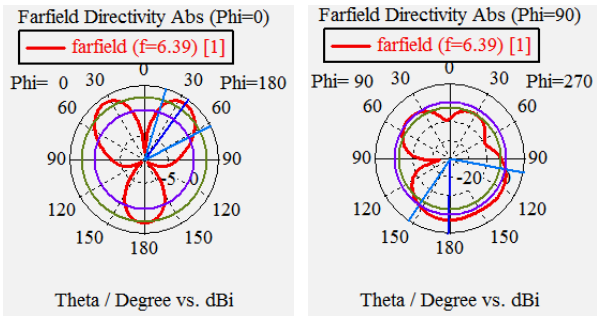

(a)

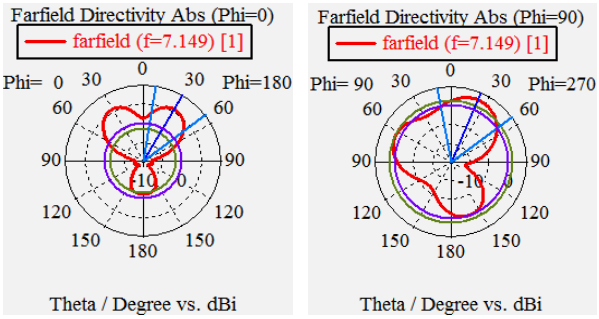

(b)

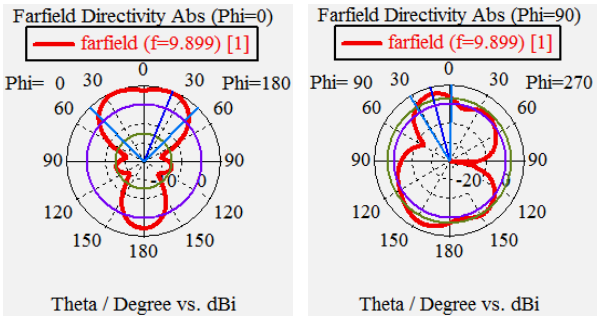

(c)

Fig. 3. Far-field radiation patterns for (a) 6.39 GHz, (b) 7.15 GHz, and (c) 9.89 GHz respectively.

B. Antenna bandwidth and return loss (S11)

Amount of power reflected from the antenna due to termination mismatch determines the performance of the designed antenna. As S_{11} become, much smaller antenna performance improves due to lower losses. In this paper, a microstrip patch with insert feed was intended. Before design modification, the notch gap, ***g*** was initially set to 1mm. An antenna bandwidth became very narrow despite good S_{11} values at some center frequencies as demonstrated in Fig. 4 (a).

In the proposed design, we reduced the size of the notch gap '***g'*** and widened the microstrip feed line (Table 1) which subsequently improved $|S_{11}|$ and antenna bandwidth as demonstrated in Fig. 4 (b).

Simulation results of the proposed design showed, free space return loss; -44.16 dB, -24.34 dB and -18.50 dB and the operational bandwidth of the antenna at the

resonant frequencies; 653.3 MHz (6.39 GHz), 1044.7 MHz (7.15 GHz) and 1775.8 MHz (9.89 GHz) respectively.

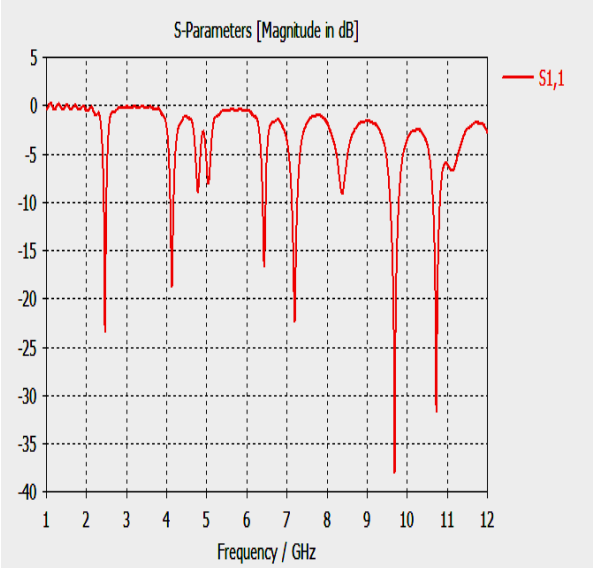

(a)

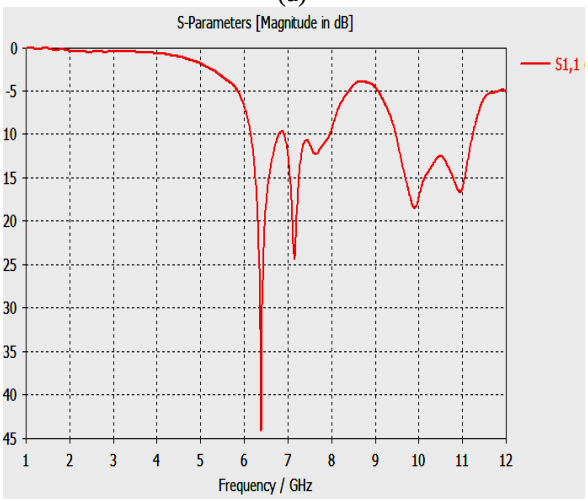

(b)

Fig. 4. Return loss (S_{11}) of the antenna: (a) based on calculation before modification, and (b) proposed antenna characteristics after modification.

C. Voltage Standing Wave Ratio (VSWR)

The quality of the antenna termination determines its reflection coefficient. Proper impedance matching at the antenna feed point (50Ω) results to lower reflection loss and subsequently the voltage standing wave ratio.

During simulation, the magnitude of the S_{11} improved proportionally with the voltage standing wave ratio. Lower VSWR shows how well the antenna impedance is matched to the transmission line characteristic impedance. Simulation results show that at the resonant frequencies the VSWR remained below standard limits (VSWR<1.5) as demonstrated in red dotted line Fig. 5.

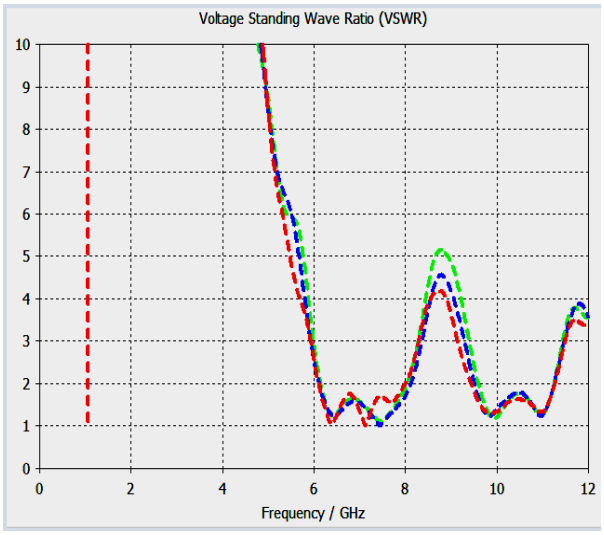

Fig. 5. VSWR values at the resonant frequencies.

Antenna dimensions, support bandwidth and return loss of the referenced design method are tabulated comparatively against the proposed model in Table 2. The antenna features varied from one another due to the type of the simulation software or slight variation of the substrate material, dielectric constant and overall antenna dimensions. Apart from the lowest dielectric constant, the thickness of the antenna remained nearly equal to those of the higher permittivity values without any performance constraints. Lower dielectric constant of the substrate material results into larger antenna size, tabulated results show that the antenna dimension remained smaller despite the analytical design requirement.

Table 2: Comparison of common antenna features

Ref. #	Substrate	Size mm^3	BW GHz	Highest S_{11} (dBm)
[9]	FR4, $\mathcal{E}_{r=4.4}$	30 x 35 x1.6	8.28	-47 (HFSS)
[12]	RT/duroid 5880, $\mathcal{E}_{r=2.2}$	38 x 50 x 1.57	4.171	-26.3 (CST)
Prop.	RT/duroid 5880, $\mathcal{E}_{r=1.96}$	40 x 45 x 1.66	3.474	-44.16 (CST)

V. CONCLUSIONS

In this work, we have designed a Triple Ultra Wide Band (Triple-UWB) patch antenna which resonates at 6.39 GHz, 7.15 GHz and 9.89 GHz. The entire cumulative bandwidth of the proposed antenna subdivides into three frequency bands (653.3 MHz, 1044.7 MHz, and 1775.8 MHz respectively) each operating at UWB. The design

approach by introducing chamfers, elliptical and circular slots on the patch with a minor rectangular aperture on the background plane has highly improved antenna radiation properties as well as the bandwidth and return loss. The three separate bands ease frequency planning and usage for various off-body WBAN applications. The notched frequency bands were under the influence of the thickness of the substrate and a very narrow notch gap. Using UWB antenna, WBAN applications can use uniform energy for signal communication which ensures reduced spectrum noises, longer network lifetime and better quality of service.

ACKNOWLEDGMENT

This research was funded by the National Key Research & Development Project, "Non-contact Noninvasive Cardiac Magnetic Resonance Imaging Diagnosis System," Project No. 2016YFC0101700.

REFERENCES

[1] M. Ghamari, B. Janko, R. S. Sherratt, W. Harwin, and R. Piechockic, "A survey on wireless body area networks for eHealthcare systems in residential environments," *Sensors*, vol. 16, no. 6, p. 831, 2016.

[2] M. Waheed, R. Ahmed, W. Ahmed, M. Drieberg and M. M. Alam, "Towards efficient wireless body area networks using two-way relay cooperation," *Sensors*, vol. 18, no. 2, p. 565, 2018.

[3] S. L. Cotton, R. D'Errico, and C. Oestges, "A review of radio channel models for Body-centric communications," *Radio Sci*., vol. 49, pp. 371-388, 2014.

[4] H. Sun, Z. Zhang, R. Q. Hu, and Y. Qian, "Wearable communications in 5G: Challenges and enabling technologies," *arXiv:*1708.05410v2 [cs.NI], 22 Dec. 2017.

[5] J. Lilja, P. Salonen, T. Kaija, and P. de Maagt, "Design and manufacturing of robust textile antennas for harsh environments," *IEEE Transactions on Antennas and Propagation*, vol. 60, no 9, Sep. 2012.

[6] M. Hamalainen, et al., "ETSI TC smart BAN: Overview of the wireless body area network standard," *15th International Symposium on Medical Information and Communication Technology (ISMICT)*, 2015.

[7] Y. Liao, M. S. Leeson, M. D. Higgins, and C. Bai, "Analysis of in-to-out wireless body area network systems: Towards QoS-aware health internet of things application," *Electronics*, vol. 5, no. 38, 2016.

[8] S. Hussain, "Current trends in antenna design for body-centric wireless communication," *International Journal of Science and Engineering Research*, ISSN 2229-5518, vol. 3, no. 6, June 2012.

[9] N. M. Award and M. K. Abdelazeez, "Multislot microstrip antenna for ultra-wideband applications," *Journal of King Saudi University of Engineering Sciences*, vol. 30, no. 1, pp. 38-45, Jan. 2018.

[10] S. Ullah, M. Ali, Md. A. Hussain, and K. Sup Kwek, "Applications of UWB Technology," *arXiv*:0911. 168v3 [cs: NI], 2 Apr. 2016.

[11] Md. S. Bin Alam and S. Moury, "Conversion of an ultra-wide band (UWB) antenna to dual band antenna for wireless body area network (WBAN) applications," *3rd International Conference on Informatics, Electronics, and Vision*, 2014.

[12] M. Turkmen and H. Yalduz, "Design and analysis of quad-band grid array microstrip antenna at UWB and ISM channel frequencies for WBAN operations," *IEEE-2017, 10th International Conference on Electrical and Electronics Engineering (ELECO)*, 2017.

[13] K. Shafique, B. A. Khawaja, M. A. Tarar, B. M. Khan, M. Mustafa, and A. Raza, "A wearable ultra-wideband antenna for wireless body area networks," *Microwave Application Technology Letters*, vol. 58, no.7, July 2016.

[14] I. Gill and F. Garcia, "Wearable PIFA antenna implemented on the jean substrate for wireless body area network," *Journal of Electromagnetic Waves and Application*s, 31:11-12, pp. 1194-1204.

[15] A. H. Bondok, A. M. El-Mohandes, A. Shalaby, and M. S. Sayed, "A low complexity UWB-PHY baseband transceiver for IEEE 802.15.6 WBAN," *IEEE-2017, 30th IEEE International System on Chip Conference (SOCC)*, 2017.

[16] A. W. Alshareefa, S. F. Amleb, N. M. Awadc, and M. K. Abdelazeezd, "UWB Antenna for WLAN band rejection," *Jordan Journal of Electrical Engineering*, vol. 4, no. 2, pp. 62-70, 2018.

[17] J. Dong, Q. Li, and L. Deng, "Compact planar ultra wide-band antenna with 3.5/5.2/5.8GHz triple band-notched characteristics for the internet of things applications," *Sensors*, vol. 17, no. 349, 2017.

[18] N. S. Reddy, K. S. Naidu, and S. A. Kumar, "Performance and design of spear-shaped antenna for UWB band applications," *Alexandria Engineering Journal*, 2017.

[19] C. Liu, Y. Guo, and S. Xiao, "review of implantable antennas for wireless biomedical devices," *Forum for Electromagnetic Research Methods and Application Technologies (FERMAT)*.

[20] A. A. Roy, J. M. Mom, and G. A Igwue, "Enhancing bandwidth of a microstrip patch antenna using slots shaped patch," *American Journal of Engineering Research (AJER)*, vol. 2, no. 9, pp. 23-30, 2013.

[21] S. Bhattacharjee, S. Maity, S. K. Metya, and H. T. Bhunia, "Performance enhancement of an implant-

able medical antenna using differential feed technique," *Engineering Science and Technology an International Journal*, vol. 19, pp. 642-650, 2016.

[22] M. Nachiappan and T. Azhagarsamy, "Design and development of dual-spiral antenna for implantable biomedical applications," *Biomedical Research*, vol. 20 no. 12, pp. 5237-5240, 2017.

[23] B. Ivsic, G. Golemac, and D. Bonefacic, "Performance of wearable antenna exposed to adverse environmental conditions," *IEEE 2013, 21st International Conference on Applied Electromagnetics and Communications (ICECom)* - Dubrovnik, Croatia (2013.10.14-2013.10.16) ICECom, 2013.

[24] P. Soontornpipit, "A dual-band compact microstrip patch antenna 403.5MHz and 2.45 GHz ISM for on-body communications," *2016 International Electrical Engineering Congress* (iEECON2016), Chiang Mai, Thailand, 2-4 Mar. 2016.

[25] M. Jahanbakht and A. A. Neyestanak, "A survey on recent approaches in the design of Band notching UWB antennas," *Journal of Electromagnetic Analysis and Applications*, 4, pp. 77-84, 2015.

[26] A. Khan and R. Nema, "Analysis of five different dielectric substrates on microstrip patch antenna," *International Journal of Computer Applications (0975-8887)*, vol. 55, no. 18, Oct. 2012.

[27] M. T. Ali, N. Ramli, M. K. M Salleh, and M. N. Md. Tan, "A design of reconfigurable rectangular microstrip patch antenna," *2011 IEEE International Conference on System Engineering and Technology (ICSET)*, 2011.

[28] S. Sharma, C. C. Tripathi, and R. Rishi, "Impedance matching techniques for microstrip patch antenna," *Indian Journal of Science and Technology*, vol. 10, no. 28, July 2017.

Kefa G. Mkongwa received his B.Eng. in Electronics and Communication Engineering and M.Eng. in Signal and Information Processing from St. Joseph University of Engineering and Technology in Tanzania and Tianjin University of Technology and Education in Tianjin, China in 2009 and 2013 respectively. He is currently pursuing Ph.D. research studies in Signal and Information Processing at Harbin Engineering University. His current area of research interests is the Internet of Things, Microstrip patch antennas, Wireless sensor networks and Wireless Body Area Networks (WBAN).

Qingling Liu received B.S. and M.S. degrees in Signals and Information Processing from the College of Information and Communication Engineering, Harbin Engineering University, Harbin, China in 2000 and 2004 respectively.

She completed her Ph.D. degree in Computer and Software Engineering, Kumoh National Institute of technology, Korea in 2012. Since 2018, she holds a Deputy Director of the Institute in the College of Information and Communication Engineering.

Her research interests include Wireless Network Technology, Internet Information Security, Artificial Intelligence, Information Technology, Routing in MANETs and Wireless Sensor Networks.

Chaozhu Zhang received his B.S. degree in Electronics and Information Engineering, M.S. degree in Communications and Information Systems and a Ph.D. degree in Signal and Information Processing from Harbin Engineering University in 1993, 2002 and 2006 respectively.

Since 2009, he has been a Professor with the Harbin Engineering University, where he now holds an Associate Dean in the College of Information and Communication Engineering. Also, he is an academician of Aerospace Society and a member of the Institute of biomedical, Heilongjiang Province.

His research interests include radar signal processing, biological signal processing, and communication engineering.